Natural Analogue Constraints on Europa's Non-ice surface Material

Journal Item

Natural analogue constraints on Europa's non-ice surface material

Mark G. Fox-Powell[1], Gordon R. Osinski[2], Daniel Applin[3], Jessica M. Stromberg[3†], Fernando Gázquez[1‡], Ed Cloutis[3], Elyse Allender[1], Claire R. Cousins[1]

[1] School of Earth and Environmental Sciences, University of St Andrews, Irvine Building, St Andrews, UK.

[2] Centre for Planetary Science and Exploration/Dept. Earth Sciences, University of Western Ontario, London, Ontario, Canada.

[3] Department of Geography, University of Winnipeg, Winnipeg, Manitoba, Canada

Corresponding author: Mark G. Fox-Powell (mgfp@st-andrews.ac.uk)

†Current address: CSIRO Mineral Resources, Perth, WA, Australia

‡ Current address: Department of Geology and Biology, University of Almería, Almería, Spain

Key Points:

- Low-temperature hydrated salts from the Canadian Arctic provide geochemical and spectral analogues for europan surface material.
- Qualitatively different deposits can form from fluids with similar major ion chemistry
- Endogenic sulfates on Europa would not rule out a chloride-dominated ocean.

Abstract

Non-icy material on the surface of Jupiter's moon Europa is hypothesised to have originated from its subsurface ocean, and thus provide a record of ocean composition and habitability. The nature of this material is debated, but observations suggest that it comprises hydrated sulfate and chloride salts. Analogue spectroscopic studies have previously focused on single phase salts under controlled laboratory conditions. We investigated natural salts from perennially cold (<0 °C) hypersaline springs, and characterised their reflectance properties at 100 K, 253 K and 293 K. Despite similar major ion chemistry, these springs form mineralogically diverse deposits, which when measured at 100 K closely match reflectance spectra from Europa. In the most sulfate-rich samples, we find spectral features predicted from laboratory salts are obscured. Our data are consistent with sulfate-dominated europan non-icy material, and further, show that the emplacement of endogenic sulfates on Europa's surface would not preclude a chloride-dominated ocean.

Plain Language Summary

Europa, a moon of Jupiter, has become a priority target in the search for life off the Earth, due to the presence of a liquid water ocean under its icy shell. Salts on the moon's surface might originate from this ocean, and therefore offer a way of studying the ocean without requiring direct access. Our knowledge of these salts comes from comparing spacecraft measurements to pure salts produced in laboratories. We have studied natural salts from hypersaline springs in the Canadian Arctic as an alternative, complementary approach. Measuring samples from these deposits at europan surface temperatures, several unexpected properties were observed, including the absence of spectral details predicted by previous laboratory studies. This challenges some of the estimates of europan surface composition. Natural analogues such as these will form part of an integrative approach to understanding data from upcoming missions, such as NASA's Europa Clipper and ESA's JUICE.

1. Introduction

In the coming decade, the European Space Agency's JUpiter ICy moons Explorer (JUICE) and the NASA Europa Clipper will study the icy moon Europa to better understand its surface and subsurface activity, and potential habitability. Europa hosts a liquid water layer beneath an icy crust (Carr et al., 1998), with a depth of up to 100 km (Nimmo & Pappalardo, 2016). The interaction between this ocean and a silicate core could generate the necessary chemical conditions for life, meaning Europa may harbour the largest habitable volume of water in the solar system (Nimmo & Pappalardo, 2016).

Constraining ocean composition is crucial to understanding the evolution and astrobiological potential of Europa. The europan surface is predominantly water ice (Carlson et al., 2009); however spatially heterogenous, non-icy material exists, first studied by the Galileo spacecraft's Near Infrared Mapping Spectrometer (NIMS) (McCord et al., 1999). This material is hypothesised to have originated, either wholly or partly, from the subsurface ocean, becoming frozen into exhumed ice or delivered directly to the surface through cryovolcanism (Schmidt et al., 2011; Prockter et al., 2017; Howell & Pappalardo, 2018). The existence of putative cryovolcanic plumes on Europa (Jia et al., 2018; Roth et al., 2014) further suggest that material from Europa's interior is actively emplaced onto the surface. This surface material can provide a record of ocean chemistry accessible to orbital or landed spacecraft.

Multiple observations of Europa's non-icy material exist, showing visible-near-infrared (vis-NIR) evidence for hydrated compounds (Brown & Hand, 2013; Carlson et al., 2005; Dalton et al., 2012; Fischer et al., 2015, 2016; Ligier et al., 2016; McCord et al., 1999). Such material can form through exogenic and radiolytic processes, salt precipitation from subsurface brines, or a combination of these two mechanisms. Previous studies have attempted to explain the shape of europan non-icy

spectra with numerical linear mixes of pure salt spectra (Carlson et al., 2005; Dalton, 2007; Ligier et al., 2016), or with experimentally-produced salt assemblages (Orlando et al., 2005). Based on these works, hydrated sulfates such as mirabilite ($Na_2SO_4.10H_2O$) and sulfuric acid hydrate have been proposed as major components of deposits on the trailing hemisphere (Carlson et al., 2005; Dalton et al., 2012; Shirley et al., 2010), whereas chloride salts may contribute to spectral signatures of 'chaos' regions (Brown & Hand, 2013; Fischer et al., 2016).

The study of natural analogues provides a complementary approach, particularly for understanding spectral behaviour of mineralogically heterogeneous precipitates. Axel Heiberg Island in the Canadian Arctic hosts unique hypersaline, sub-zero (< 0 °C) springs that precipitate hydrated sodium sulfates and chloride salts, along with other low temperature phases (Battler et al., 2013; Ward & Pollard, 2018). We investigated the vis-NIR spectral properties and geochemical context of these natural hydrated salt assemblages and discuss their relevance for the exploration of Europa.

2. Field Areas

Axel Heiberg Island (AHI), Nunavut, Canada (Fig. 1A) hosts Carboniferous evaporite diapirs (Harrison & Jackson, 2014) and thick (> 400 m) permafrost (Andersen et al., 2002). Associated with the diapirs are anoxic, perennially low-temperature (-5–8 °C) hypersaline (> 10 wt. %) springs that form assemblages of hydrated sulfate and chloride salts (Battler et al., 2013; Pollard et al., 1999). The precipitation of these Europa-relevant phases makes these springs compelling natural laboratories for understanding analogous deposits on Europa. The waters of three springs, Lost Hammer, Colour Peak and Stolz, were sampled along with their associated salt deposits in July

2017 (Fig. 1) (for further details of geologic setting see Battler et al., 2013, Ward and Pollard, 2018).

2.1 Lost Hammer

Lost Hammer (LH) Spring (also known as Wolf Spring; Battler et al., 2013) (79.076856, -90.210472) emerges as a single outlet from the valley floor, approximately 500 m from the base of Wolf Diapir (Fig. 1B). A large dome of salt exists around the vent, flanked by a salt apron with terracing and layering. Brine samples and measurements were taken from the outlet, and at two downstream points. Salt samples were taken from within the outlet dome and from the salt apron (Fig. S1).

2.2 Colour Peak

Colour Peak (CP) springs (79.38, -91.27) emerge as several outlets from the side of Colour Peak Diapir (Fig. 1C). Precipitates exist as sintered terraces exhibiting green and black colouration. White crusts are visible at the edges of channels and pools. Brine samples and measurements were taken at five spring outlets, and mineral samples were taken from terraces and peripheral precipitates (Fig. S1).

2.3 Stolz

Stolz (STZ) springs (79.090117, -87.048248) emerges from two outlets on Stolz Diapir (Fig. 1). The springs meet at a confluence 20 m downstream from the outlets, precipitating an extensive

salt apron with an approximate thickness of 5 m and downslope extent of ~800 m. During summer, the drainage streams flow under this apron into a 'salt cave'. Salts form grey and white terraces (Fig. 1E), with the dry remains of large (~10 m diameter) pools on the apron. Brine samples and measurements were taken at both outlets and at the confluence. Salts were sampled at the entrance to the salt cave and from the apron surface (Fig. S1).

3. Materials and methods

3.1 Sampling

Brine samples were 0.22 µm-filtered into four 15 ml aliquots for stable isotopes, anion and cation analysis, and aqueous sulfide measurements. Samples for cation analyses were acidified to a final concentration of 1 % HNO_3. Temperature, pH and dissolved oxygen (DO) concentrations were measured using a Mettler Toledo FiveGo probe. Salt mineral precipitates were collected into sample bags and stored at ambient arctic temperatures, shipped chilled (4 °C), and stored at 4 °C until analysis.

3.2 Quantification of major ions

Cations in spring fluids were measured with ICP-AES using a Prodigy7 (Teledyne-Leeman) AES system at the Open University, UK. Chloride and sulfate were measured in triplicate with ion-chromatography using a Metrohm 930 IC system fitted with a 150 mm Metrosep Asupp5 separation column (4 mm bore). Relative standard deviations of triplicate measurements were ≤0.1 % for all measured anions. Brines were diluted by a factor between 10^3 and 10^4 in ultrapure

136 deionised water prior to analysis. Aqueous sulfide was quantified spectrophotometrically in
137 triplicate using the methylene blue assay (Cline, 1969).

138

139 **3.3 Oxygen and hydrogen isotopes in waters**

140 Water-bound ^{16}O, ^{18}O, H, and D were measured simultaneously by cavity ringdown spectrometry
141 using a L2140-i Picarro water isotope analyser at the University of St. Andrews, United Kingdom.
142 Seven repeat measurements were averaged for each sample, with a typical precision of ±0.013 ‰
143 (1 SD.). See supplementary methods for more details.

144

145 **3.4 X-ray diffraction (XRD)**

146 Powder XRD patterns were recorded at Drochaid Research Services, Ltd. (St Andrews, UK) at
147 room temperature from 10° to 110° (2θ) using a Panalytical X'Pert Pro X-ray diffractometer.
148 Samples were equilibrated to room temperature and crushed as finely as possible prior to analysis.
149 In an effort to retain hydrated phases, samples were not fully dried, therefore sieving and grain
150 size normalisation was not possible. Because of this, Rietveld refinements are taken as semi-
151 quantitative, indicative of major and minor phases. See supplementary methods for more details.

152

153 **3.5 Visible-near-infrared reflectance spectroscopy**

154 Vis-NIR (0.35 to 2.5 μm) spectra from salt precipitates were collected at three temperatures: 293
155 K (room temperature), 253 K and approximately 100 K (simulating europan surface temperature;
156 Nimmo and Pappalardo, 2016). Spectra were acquired with an Analytical Spectral Devices

157 FieldSpec Pro HR spectrometer at the Planetary Spectroscopy Facility, University of Winnipeg.
158 See supplementary methods for more details. Samples at 253 K were frozen in a chest freezer,
159 followed by active cooling with a Pelletier cooler after Bramble et al. (2014). Samples measured
160 at 100 K were held in an aluminium sample cup that was immersed in liquid nitrogen and
161 equilibrated until the liquid nitrogen ceased to boil vigorously.

162 The 100 K spectra were resampled to (1) Galileo NIMS spectral resolution, to precisely match
163 bandpasses in the G1ENNHILAT01 observation presented by Dalton et al. (2005) and others; (2)
164 the Europa Clipper Mapping Infrared Spectrometer for Europa (MISE) spectral resolution (10 nm
165 sampling from 0.8-5 μm) (Blaney et al., 2015), and (3) the JUICE Moons and Jupiter Imaging
166 Spectrometer (MAJIS) spectral resolution (2.3 nm sampling from 0.4-1.7 μm; 6.6 nm sampling
167 from 1.7-5.7 μm) (Langevin et al., 2013).

168

169 **3.6 Spectral mixing**

170 To investigate the loss of spectral detail caused by the presence of anhydrous phases, linear spectral
171 mixes were generated to compare directly with the LH outlet sample, which has four phases in
172 XRD patterns: anhydrous thenardite (Na_2SO_4) and halite (NaCl), and their hydrous counterparts
173 mirabilite ($Na_2SO_4.10H_2O$) and hydrohalite ($NaCl.2H_2O$). Semi-quantitative XRD indicates
174 sulfates form the major salt phase (approximately 80%) with a minor chloride salt phase
175 (approximately 20%), and this ratio was maintained in each mix, varying the anhydrous component
176 from 0% (fully hydrated; i.e. mirabilite and hydrohalite) to 100% (fully anhydrous; i.e. thenardite
177 and halite). Pure phase spectra were taken from Hanley et al. (2014), Shirley et al. (2010) and the
178 USGS spectral library (Supplementary Methods).

4. Results

4.1 Aqueous geochemistry and salt mineralogy

Brine compositions and salt mineralogy at the springs are consistent with published data (Battler et al., 2013; Lay et al., 2013; Omelon et al., 2006; Ward & Pollard, 2018). Across all springs, fluids are dominated by sodium and chloride and contain significant concentrations of sulfate (Fig. 2A; Table S1). LH brines contain the highest sulfate concentration of the three springs (60 mM), and the lowest temperature (-3.6 °C). CP brines are relatively warm (3.8-8.4 °C), neutral alkaline (pH 6.98-7.75) and contain higher dissolved Ca^{2+} levels than either LH or STZ (Fig. 2B; Table S1). STZ brines are the most saline with respect to sodium (3790-3868 mM) and chloride (5213-5216 mM) and possess sub-zero temperatures (-1.7 and -2.9° C). Sulfide concentrations ranged from highs of 1.86 mM at CP to lows of 0.04 mM at STZ (Table S1). The δD and $\delta^{18}O$ of the spring brines plot close to the local meteoric water line (LMWL) (Fig. 2C). LH brine shows the lowest $\delta^{18}O$ and δD values of the springs but is comparable to that of nearby permafrost. CP brine isotope values plot close to snowmelt on Colour Peak Diapir, in agreement with Pollard et al. (1999) (Fig. 2C). The isotopic values of two snowmelt pools sampled on Stolz Diapir fall below the LMWL and show higher $\delta^{18}O$ and δD than the STZ brines (Fig. 2C).

Mineralogy (measured by XRD after raising samples to 20 °C) is dominated at LH by Na-sulfates, notably mirabilite and thenardite, with lesser contributions from chlorides (Table S2). The low-temperature chloride hydrohalite is present in several samples, which had not previously been reported by Battler et al. (2013). White crusts at CP are dominated by halite, while dark precipitates consisted primarily of gypsum ($CaSO_4.2H_2O$) and calcite ($CaCO_3$), which are not considered likely phases at Europa. White salt assemblages at STZ contained higher abundances of Na-chloride

salts, predominantly anhydrous halite. The darker banded salts were composed of thenardite and halite, as approximately equal major phases.

4.2. Visible-near-infrared spectral characteristics

Representative spectra from salt precipitates at all three measured temperatures are plotted in Fig. 3. The largest spectral differences are observed between 253 K and 273 K. 'CP-green' (dark green precipitates) show a sharpening of the major water absorption bands at 1.5 (triplet), 2.0 (doublet) and 2.2 µm (triplet) at 253 and 100 K, consistent with gypsum (Cloutis et al., 2006), which dominates this sample (Table S2) and is stable at room temperature. Spectra from 'STZ-white' at 253 K and 100 K are consistent with hydrohalite; particularly the doublet 1.5 and 2.0 µm features (Light et al., 2016; measured at 243 K), and the 1.75 µm feature in frozen NaCl brine (Hanley et al., 2014). 'STZ-dark' salts display muted versions of these features. Spectra from CP-white, and all LH and STZ salts have minimal hydration features at 293 K, with overtone absorptions at 1.2 and 2.2 µm absent entirely. LH spectra exhibit the 2.2 µm absorption feature as a slight shoulder to the larger and broader 2.0 µm feature, consistent with the presence of mirabilite. Salts from the interior of the outlet dome show broader absorptions, and exhibit hydration features at 1.0 and 1.2 µm that are absent in salts from the surface of the salt apron. Numerical linear mixes failed to recreate LH spectra, even when all components identified by XRD were included (Fig. 4). For example, hydrohalite details were not observed in LH spectra, but were evident in spectral mixes designed to simulate LH phase abundances.

4.3. Comparisons with mission data

100 K spectra resampled to match spacecraft instrument capabilities are plotted in order of decreasing resolution in Fig. 3C, D. Major absorption features in LH salts show similar asymmetry and broadening to the NIMS data from europan non-icy material. Furthermore, minima for the 1.75 µm band in LH salts very closely matches the corresponding minimum of Europa's non-icy material observed by NIMS. Band minima of the major 1.5 and 2.0 µm absorptions tend to shift to shorter wavelengths at lower spectral resolution (Fig. 3D). Spectral details such as the diagnostic gypsum triplets in CP salts and the hydrohalite doublets in STZ salts (1.5, 2.0 µm) are represented at MISE and MAJIS resolutions, but at NIMS resolution these become difficult to resolve or are absent entirely. The hydrohalite doublet at 2.0 µm in STZ-white appears as a single feature at NIMS resolution with a band minimum that closely matches data from Europa.

5. Discussion

5.1. Environmental controls on spring geochemistry

The AHI springs provide geochemical analogues for the formation of hydrated salt deposits from subsurface fluids on icy moons. Constraining their geologic and geochemical context as well as their stability is crucial for understanding which aspects can be extrapolated for planetary exploration. The brine $\delta^{18}O$ and δD values support the hypothesis that the AHI springs are recharged by meteoric water. Anderson et al. (2002) suggested that evaporite diapirs create conduits through permafrost that allow meteoric waters to infiltrate and dissolve deep evaporites,

buffering the spring temperatures via a dynamic equilibrium between the sub-permafrost geotherm and the permafrost itself. The behaviour of the STZ and LH systems are consistent with this idea. At both sites, $\delta^{18}O$ and δD values of the spring brines are significantly more depleted than local snowmelt, and at LH are similar to permafrost values. This indicates a complex mechanism of water recharge to the system, potentially including local permafrost melts and more distal meteoric sources that could have experienced a longer residence time in the evaporites. At CP however, similar δD and $\delta^{18}O$ values in the brine and snow show that contemporary melt is likely feeding the springs, consistent with interpretations by Omelon et al. (2006). This challenges the notion (Pollard et al., 1999) that long residence times are required within the evaporites and permafrost to acquire a high solute load and to buffer the spring temperatures.

5.2 Implications for spectroscopic detection of salts on Europa

The natural salts studied here show complex behaviours, not fully predictable from the behaviours of pure laboratory salts. Some samples, notably CP-green, CP-white and STZ-white, show sharpening of spectral detail at 253 and 100 K, predicted from pure salts. However, for most samples the main temperature-related spectral changes are associated with the loss of hydration at 293 K, and not the narrowing or sharpening effects seen at low temperature with pure salts. For example, the mirabilite-dominated LH salts lack the sharpened details observed in pure mirabilite (Dalton et al., 2005), instead exhibiting smooth absorptions that span the 1.3-1.7 and 1.8-2.3 μm ranges. Achieving this 'smoothing' effect in previous linear mixing efforts was achieved by adding up to 65 % sulfuric acid hydrate (Carlson et al., 2005; Dalton et al., 2012). Based on LH salt spectra, which contain only Na-sulfates and chloride salts (plus trace detrital quartz), 'smooth' low temperature spectra do not require the addition of sulfuric acid hydrate. This does not rule out its

265 presence at Europa, but demonstrates it need not be such a significant component to produce the
266 observed spectral features.

267 Overall, LH salt spectra measured at 100 K most closely recreate the shape, breadth and depth of
268 absorption features in NIMS non-icy spectra, including the 1.75 µm band minimum (Fig. 3D).
269 These data therefore are consistent with an LH-like sulfate-rich composition at Europa. However,
270 they do not rule out the presence of chlorides salts, as data from Europa show some similarity to
271 the chloride-rich STZ samples when viewed at the lower spectral resolution of mission data. The
272 hydrohalite doublet at 2.0 µm in STZ-white disappears at NIMS resolution, meaning that this
273 feature would not have been detectable, even if hydrohalite were present. Recent ground-based
274 observations with greatly improved spectral resolution (*e.g.*, Fischer et al., 2015) lack data in the
275 1.80-1.95 µm region, so also cannot be used to definitively eliminate hydrohalite. Future spacecraft
276 instruments such as MISE (Europa Clipper) and MAJIS (JUICE) have sufficient resolution to
277 capture this, and other diagnostic features, therefore these missions will reveal if europan non-icy
278 deposits bear closer resemblance to a "LH-" or "STZ-like" composition.

279 Hydrohalite was detected in some LH samples by XRD (Table S2) as a minor phase, including
280 LH-outlet. Spectral linear mixing predicts that hydrohalite should be observable in the near-
281 infrared in this sample, however apart from a subtle reflectance minimum at 1.983 µm, hydrohalite
282 features were absent, even when the sample was measured at 100 K (Fig. 4). Incorporating
283 spectrally featureless anhydrous phases at proportions above 50% into the mix produces similar
284 smoothing effects, but causes features at 1.5 and 2.0 µm to lack the depth and breadth observed in
285 LH-outlet spectra (Fig 4b). Moreover the approximate anhydrous proportion measured by XRD at
286 room temperature (20%) provides an upper limit on anhydrous phase abundance in LH-outlet
287 material, which will be heavily hydrated at 100 K. This demonstrates that the behaviour of natural

assemblages, which can be complex intimate mixtures of compounds and hydrations states, cannot be predicted from the additive properties of pure salts alone. If ocean-derived hydrated chlorides are present on the surface of Europa (Brown and Hand, 2013), they could be spectrally obscured by sulfates. Importantly, if sulfates are exogenic in origin (i.e., from Io's plasma torus), this could present a problem for identifying endogenic material within surface deposits. In this case, the 1.983 μm band minimum could be an important diagnostic feature of hydrohalite that is retained, albeit subtly, in sulfate deposits.

5.3 Geochemical implications for Europa from natural analogues

The deposits at AHI springs show that natural brines with similar major ion chemistry can precipitate different mineralogical deposits, ranging from calcite and gypsum at CP, to mirabilite and hydrohalite at LH. These differences are accounted for by minor variations in the sulfate:chloride ratio of the brines, and by dissolved calcium and alkalinity (Fig. 2; Fig S2). CP exhibits minerals not considered likely at Europa, however their formation demonstrates how minor differences in geochemistry can produce varied mineralogies. The same may be true on a geologically diverse world such as Europa. Additionally, CP can be a useful analogue for cryovolcanic precipitates on bodies with more alkaline and carbonate-rich aqueous chemistries, such as Enceladus (Glein et al., 2015).

The compositions of AHI deposits do not reflect equilibrium salt assemblages that would form if the spring brines fully crystallised, rather they represent a snapshot during this evolution (Fig. S2; Table S3). For example, despite bearing a high chloride : sulfate ratio (25; Table S1), LH salts are dominated by mirabilite and thenardite, showing that a dominantly chloride brine can form sulfate-

dominated deposits. Thermodynamic models show that mirabilite forms early upon freezing or evaporation-driven concentration, while chlorides are retained in late-stage brines that can be transported away from the deposit (Fig. S2). On Europa, a chloride-dominated ocean in which sulfate is only a minor constituent may form sulfate-rich salt assemblages in a similar manner, at the surface or within the ice, while denser chloride-enriched brines migrate away (Zolotov & Shock, 2001). The discovery of endogenous sulfate salts on Europa would therefore not preclude a chloride-dominated ocean.

The composition of Europa's ocean is not well constrained, and the relative contributions of exogenic and endogenic processes to surface non-ice material are not known. Different geographical regions may harbour different compositions, reflecting different processes (Fischer et al., 2015). In one proposed scenario, chloride-dominated subsurface fluids are delivered to the surface and become progressively altered by exogenous sulfur ion bombardment (Brown and Hand, 2013). Under these circumstances, STZ-white salts represent pristine deposits, with STZ-dark and the LH salt assemblages representing more altered, sulfate-rich deposits where the vis-NIR signature of hydrohalite is obscured. Alternatively, if the ocean is sulfate-rich, (Kargel et al., 2000) then LH salts would represent suitable analogue material for pristine endogenic deposits. The study of natural environments such as the AHI springs forms part of an integrative theoretical, experimental and analogue approach that will be critical to interpreting future mission data, both from upcoming fly-by missions as well as the under-development NASA Europa Lander project.

Acknowledgements

This work was funded by The Leverhulme Trust (RPG-2016-153) and the Natural Sciences and Engineering Research Council of Canada. The Planetary Spectroscopy Facility, University of

Winnipeg, is supported by the University of Winnipeg, the Canada Foundation for Innovation, the Manitoba Research Innovation Fund and the Canadian Space Agency. Thanks to The Polar Continental Shelf Program (Natural Resources Canada) for logistical field support in Nunavut. Geochemical and spectral data presented in this manuscript are available in Supporting information. Finally, we thank two anonymous reviewers for constructive comments.

6. References

Andersen, D. T., Pollard, W. H., McKay, C. P., & Heldmann, J. (2002). Cold springs in permafrost on Earth and Mars. *Journal of Geophysical Research*, *107*(E3). doi:10.1029/2000JE001436

Battler, M. M., Osinski, G. R., & Banerjee, N. R. (2013). Mineralogy of saline perennial cold springs on Axel Heiberg Island, Nunavut, Canada and implications for spring deposits on Mars. *Icarus*, *224*(2), 364–381. doi:10.1016/j.icarus.2012.08.031

Blaney, D. L., Clark, R., Dalton, J. B., Davies, A. G., Green, R., Hedman, M., et al. (2015) Mapping Imaging Spectrometer for Europa (MISE). Paper presented at European Planetary Science Congress, Nantes, France

Bramble, M. S., Flemming, R. L., Hutter, J. L., Battler, M. M., Osinski, G. R. & Banerjee, N. R. (2014). A temperature-controlled sample stage for in situ micro-X-ray diffraction: Application to Mars analog mirabilite-bearing perennial cold spring precipitate mineralogy. *American Mineralogist*, *99*, 943–947. doi:10.2138/am.2014.4629

Brown, M. E., & Hand, K. P. (2013). Salts and radiation products on the surface of Europa. *The Astronomical Journal*, *145*, 110–7. doi:10.1088/0004-6256/145/4/110

355 Carlson, R. W., Anderson, M. S., Mehlman, R., & Johnson, R. E. (2005). Distribution of hydrate
356 on Europa: Further evidence for sulfuric acid hydrate. *Icarus*, *177*(2), 461–471.
357 doi:10.1016/J.ICARUS.2005.03.026

358 Carlson, R. W., Calvin, W. M., Dalton, J. B., Hansen, G. B., Hudson, R. L., Johnson, R. E., et al.
359 (2009). Europa's Surface Composition. In R. T. Pappalardo, W. B. Mckinnon, & K. Khurana
360 (Eds.), *Europa* (pp. 283–327). University of Arizona Press.

361 Carr, M. H., Belton, M. J., Chapman, C. R., Davies, M. E., Geissler, P., Greenberg, R., et al.
362 (1998). Evidence for a subsurface ocean on Europa. *Nature*, *391*, 363–365. doi:10.1038/34857

363 Cloutis, E. A., Hawthorne, F. C., Mertzman, S. A., Krenn, K., Craig, M. A., Marcino, D., et al.
364 (2006). Detection and discrimination of sulfate minerals using reflectance spectroscopy. *Icarus*,
365 *184*, 121-157. doi:10.1016/j.icarus.2006.04.003

366 Dalton, J. B. (2007). Linear mixture modeling of Europa's non-ice material based on cryogenic
367 laboratory spectroscopy. *Geophysical Research Letters*, *34*(21), 2–5. doi:10.1029/2007GL031497

368 Dalton, J. B., Prieto-Ballesteros, O., Kargel, J. S., Jamieson, C. S., Jolivet, J., & Quinn, R. (2005).
369 Spectral comparison of heavily hydrated salts with disrupted terrains on Europa. *Icarus*, *177*, 472–
370 490. doi:10.1016/j.icarus.2005.02.023

371 Dalton, J. B., Shirley, J. H., & Kamp, L. W. (2012). Europa's icy bright plains and dark linea:
372 Exogenic and endogenic contributions to composition and surface properties. *Journal of*
373 *Geophysical Research: Planets*, *117*(E03003). doi:10.1029/2011JE003909

374 Doran, P. T., McKay, C. P., Adams, W. P., English, M. C., Wharton, R. A., & Meyer, M. A.
375 (1996). Climate forcing and thermal feedback of residual lake-ice covers in the high Arctic.

Limnology and Oceanography, *41*(5), 839–848. doi:10.4319/lo.1996.41.5.0839

Fischer, P. D., Brown, M. E., & Hand, K. P. (2015). Spatially resolved spectroscopy of Europa: The distinct spectrum of large-scale chaos. *The Astronomical Journal*, *150*(164). doi:10.1088/0004-6256/150/5/164

Fischer, P. D., Brown, M. E., Trumbo, S. K., & Hand, K. P. (2016). Spatially resolved spectroscopy of Europa's large-scale compositional units at 3–4 μm with Keck NIRSPEC, *153*(13). doi:10.3847/1538-3881/153/1/13

Glein, C. R., Baross, J. A., & Waite, J. H. (2015). The pH of Enceladus' ocean. *Geochimica et Cosmochimica Acta*, *162*, 202–219. doi:10.1016/j.gca.2015.04.017

Hand, K. P., & Carlson, R. W. (2015). Europa's surface color suggests an ocean rich with sodium chloride. *Geophysical Research Letters*, *42*, 3174–3178. doi:10.1002/2015GL063559

Hanley, J., Dalton, J. B., Chevrier, V. F., Jamieson, C. S., & Barrows, R. S. (2014). Reflectance spectra of hydrated chlorine salts: The effect of temperature with implications for Europa. *Journal of Geophysical Research: Planets*, *119*(11), 2370–2377. doi:10.1002/2013JE004565

Harrison, J. C., & Jackson, M. P. A. (2014). Exposed evaporite diapirs and minibasins above a canopy in central Sverdrup Basin, Axel Heiberg Island, Arctic Canada. *Basin Research*, *26*(4), 567–596. doi:10.1111/bre.12037

Howell, S. M & Pappalardo, R. T. (2018) Band formation and ocean-surface interaction on Europa and Ganymede. *Geophysical Research Letters, 45(10)*, 4701-4709. doi:10.1029/2018GL077594

Jia, X., Kivelson, M. G., Khurana, K. K., & Kurth, W. S. (2018). Evidence of a plume on Europa from Galileo magnetic and plasma wave signatures. *Nature Astronomy*, *2*(6), 459–464.

doi:10.1038/s41550-018-0450-z

Kargel, J. S., Kaye, J. Z., Head, J. W. III, Marion, G. M., Sassen, R., Crowley, J. K., Ballesteros, O. P., Grant, S. A. & Hogenboom, D. L. Europa's crust and ocean: Origin, composition, and the prospects for life. *Icarus 148,* 226-265. doi:10.1006/icar.2000.6471

Langevin, Y., Piccioni, G. & the MAJIS Team. (2013) MAJIS (Moons and Jupiter Imaging Spectrometer) for JUICE: objectives for the Galilean satellites. Paper presented at European Planetary Science Conference, London, United Kingdom

Lay, C.-Y., Mykytczuk, N. C. S., Yergeau, É., Lamarche-Gagnon, G., Greer, C. W., & Whyte, L. G. (2013). Defining the Functional Potential and Active Community Members of a Sediment Microbial Community in a High-Arctic Hypersaline Subzero Spring. *Applied and Environmental Microbiology*, *79*(12), 3637–3648. doi:10.1128/AEM.00153-13

Light, B., Brandt, R. E., & Warren, S. G. (2009). Hydrohalite in cold sea ice: Laboratory observations of single crystals, surface accumulations, and migration rates under a temperature gradient, with application to "Snowball Earth." *Journal of Geophysical Research, 114*(C07018). doi:10.1029/2008JC005211

Light, B., Carns, R. C., & Warren, S. G. (2016). The spectral albedo of sea ice and salt crusts on the tropical ocean of Snowball Earth: 1. Laboratory measurements. *Journal of Geophysical Research: Oceans*, *121*(7), 4966–4979. doi:10.1002/2016JC011803

Ligier, N., Poulet, F., Carter, J., Brunetto, R., & Gourgeot, F. (2016). VLT/SINFONI observations of Europa: New insights into the surface composition. *The Astronomical Journal*, *151*(163) doi: 10.3847/0004-6256/151/6/163

418 Marion, G .M. & Kargel, J. S. (2008) Cold Aqueous Planetary Geochemistry with FREZCHEM.
419 *Advances in Astrobiology and Biogeophysics*. Springer-Verlag Berlin Heidelberg

420

421 McCord, T. B., Hansen, G. B., Matson, D. L., Johnson, T. V, Crowley, J. K., Fanale, F. P., et al.
422 (1999). Hydrated salt minerals on Europa's Surface from the Galileo near-infrared mapping
423 spectrometer (NIMS) investigation. *Journal of Geophysical Research*, *104*, 11827–11851.
424 doi:10.1029/1999JE900005

425 Nimmo, F., & Pappalardo, R. T. (2016). Ocean worlds in the outer solar system. *Journal of*
426 *Geophysical Research: Planets*, *121*(8), 1378–1399. doi:10.1002/2016JE005081

427 Omelon, C. R., Pollard, W. H., & Andersen, D. T. (2006). A geochemical evaluation of perennial
428 spring activity and associated mineral precipitates at Expedition Fjord, Axel Heiberg Island,
429 Canadian High Arctic. *Applied Geochemistry*, *21*(1), 1–15. doi:10.1016/j.apgeochem.2005.08.004

430 Orlando, T. M., McCord, T. B., & Grieves, G. A. (2005). The chemical nature of Europa surface
431 material and the relation to a subsurface ocean. *Icarus*, *177*(2), 528–533.
432 doi:10.1016/j.icarus.2005.05.009

433 Pollard, W., Omelon, C., Anderson, D., & McKay, C. (1999). Perennial spring occurrence in the
434 Expedition Fiord area of western Axel Heiberg Island, Canadian High Arctic. *Canadian Journal*
435 *of Earth Science*, *36*, 105–120. doi:10.1139/e98-097

436 Prockter, L. M., Shirley, J. H., Dalton, J. B. & Kamp, L. (2017) Surface composition of pull-apart
437 bands in Argadnel Regio, Europa: Evidence of localized cryovolcanic resurfacing during basin
438 formation. Icarus 285, 27-42. doi:10.1016/j.icarus.2016.11.024

Rodriguez-Navarro, C., Doehne, E., & Sebastian, E. (2000). How does sodium sulfate crystallize? Implications for the decay and testing of building materials. *Cement and Concrete Research, 30*, 1527–1534. doi:10.1016/S0008-8846(00)00381-1

Roth, L., Saur, J., Retherford, K. D., Strobel, D. F., Feldman, P. D., McGrath, M. A., & Nimmo, F. (2014). Transient Water Vapor at Europa's South Pole. *Science*, *343*(6167), 171–174. doi:10.1126/science.1247051

Schmidt, B. E., Blankenship, D. D., Patterson, G. W. & Schenk, P. M. (2011) Active formation of 'chaos terrain' over shallow subsurface water on Europa. Nature 479, 502-505.

Shirley, J. H., Dalton III, J. B., Prockter, L. M., & Kamp, L. W. (2010). Europa's ridged plains and smooth low albedo plains: Distinctive compositions and compositional gradients at the leading side-trailing side boundary. *Icarus, 210*, 358–384. doi:10.1016/j.icarus.2010.06.018

Ward, M. K., & Pollard, W. H. (2018). A hydrohalite spring deposit in the Canadian high Arctic: A potential Mars analogue. *Earth and Planetary Science Letters*, *504*, 126–138. doi:10.1016/J.EPSL.2018.10.001

Zolotov, M. Y., & Shock, E. L. (2001). Composition and stability of salts on the surface of Europa and their oceanic origin. *Journal of Geophysical Research: Planets*, *106*(E12), 32815–32827. doi:10.1029/2000JE001413

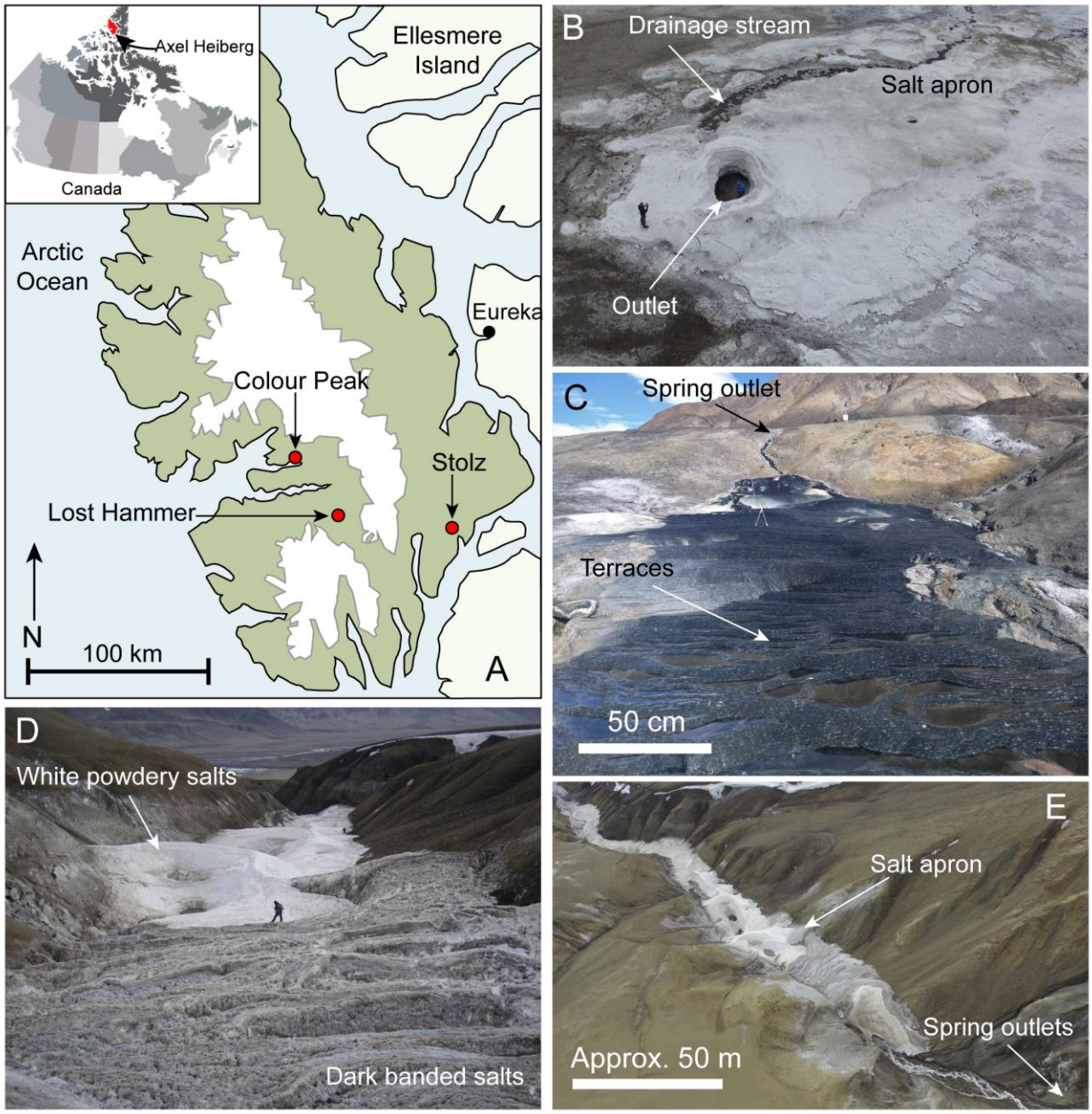

457

458 **Fig. 1: (a)** Map of Axel Heiberg Island, location of the three springs studied, and icecaps (white).

459 **(b)** Aerial view of Lost Hammer spring, showing outlet and salt apron. Person for scale. **(c)**

460 Terraces at Colour Peak springs and outlet channel. **(d)** Salt apron at Stolz Spring. Person for scale.

461 **(e)** Aerial view of Stolz Springs, showing the outlets on the side of Stolz Diapir

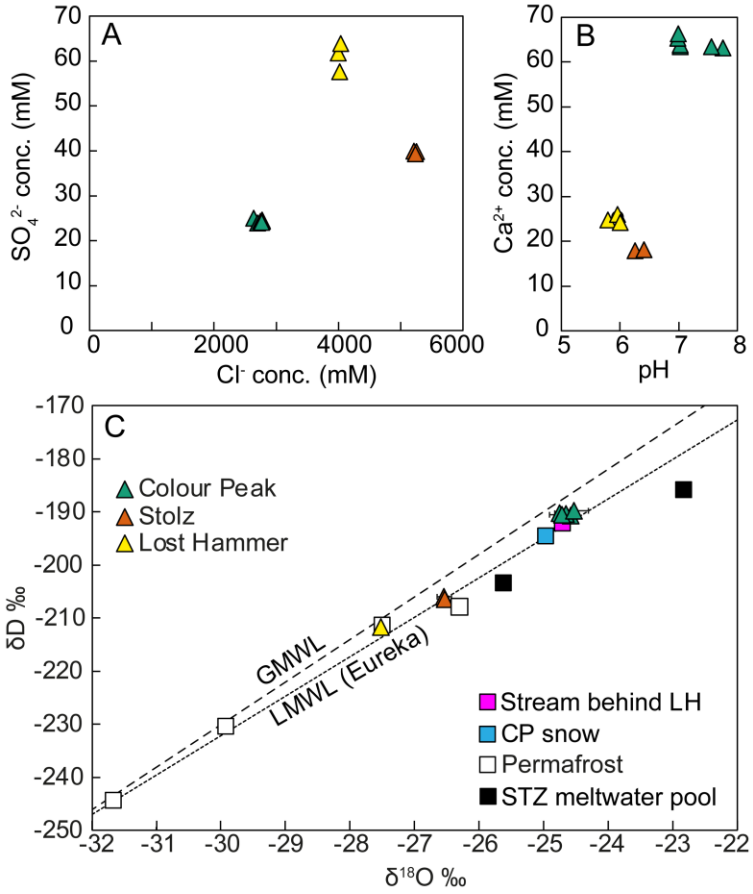

Figure 2: AHI spring geochemistry. **(a)** Major anions; **(b)** Calcium concentration vs. pH; **(c)** Water isotopic composition of the springs and potential source waters. Global (G) and local (L) meteoric water lines (MWL) plotted for reference (Pollard et al., 1999).

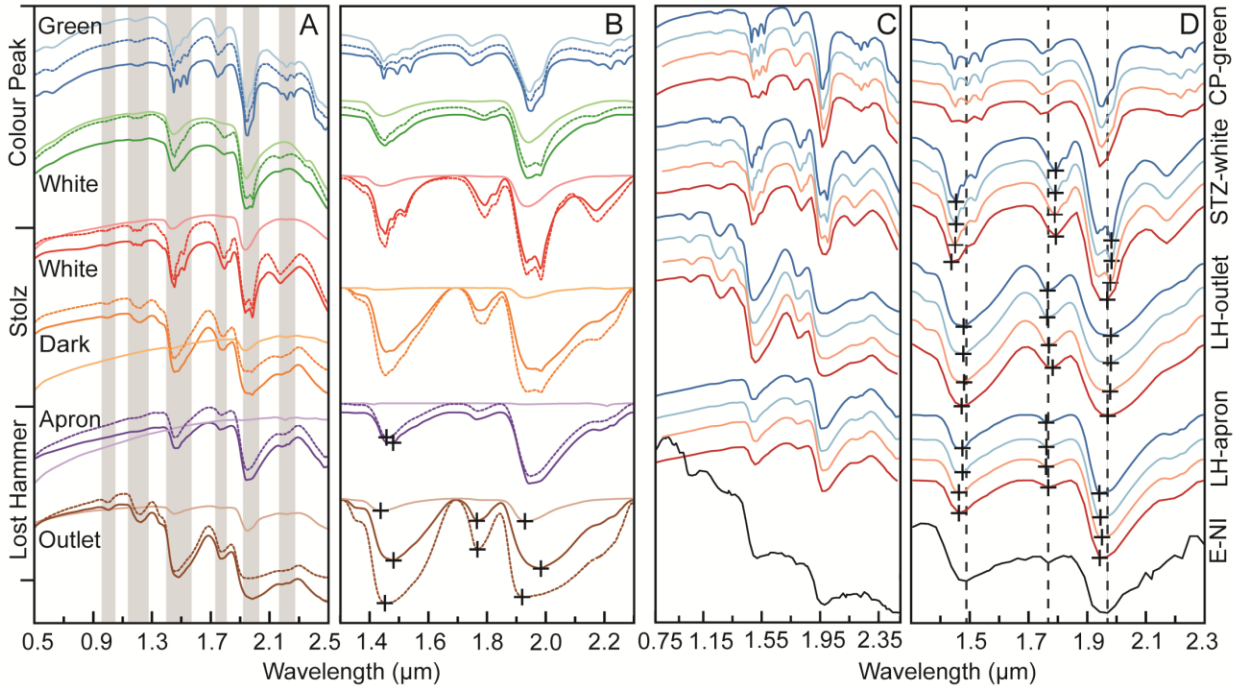

Figure 3: Representative vis-NIR reflectance spectra of salts from the AHI saline springs. Reflectance offset for clarity. **(a-b):** Full (a) and continuum-removed (b) spectra at 100 K (darkest), 253 K (dashed) and 293 K (lightest). Grey lines highlight H_2O/OH water bands. **(c-d):** Representative full (c) and continuum-removed (d) spectra resampled to instrument bandpasses, ordered from top to bottom: full nm-resolved spectra, MAJIS resolution, MISE resolution, NIMS resolution. Europa non-icy endmember spectrum (black), acquired by Galileo NIMS, is reproduced from Carlson et al. (2005). Dashed lines and crosses in (b) and (d) show the positions of absorption band minima for NIMS data and AHI data, respectively.

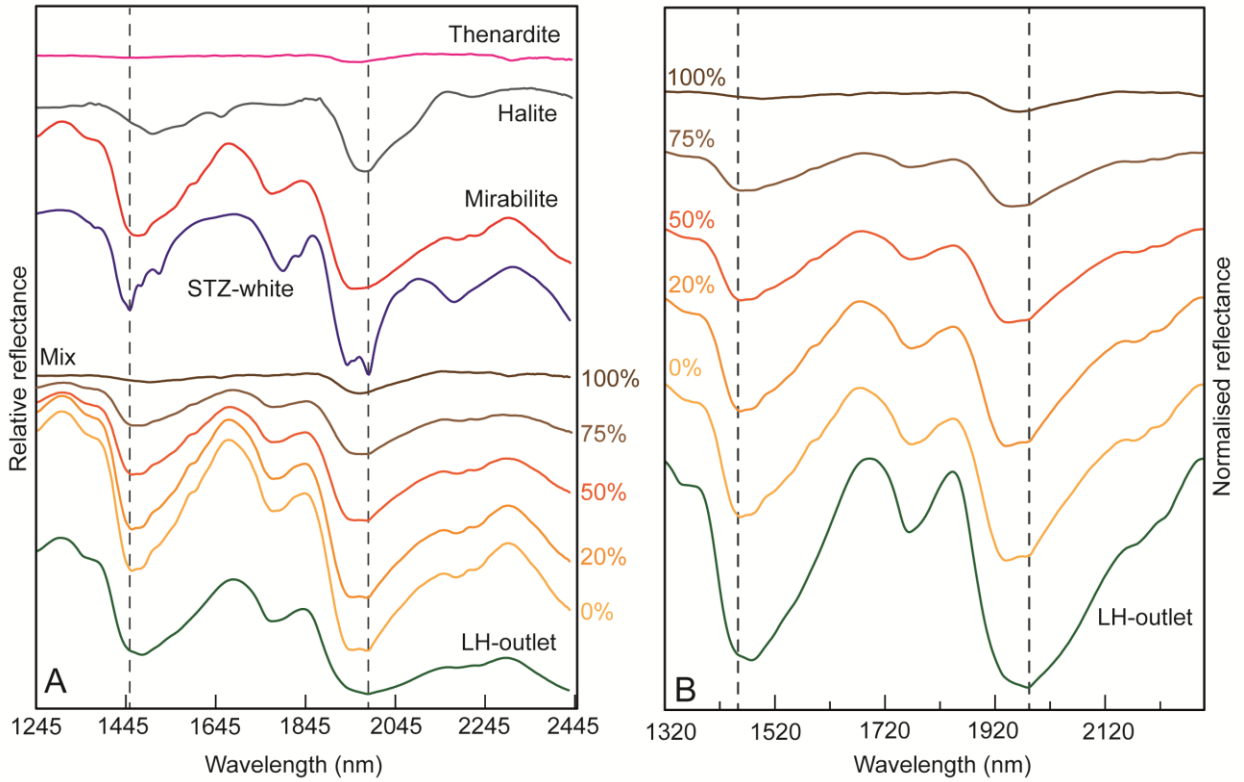

Figure 4: Comparison of numerically mixed spectra with LH-outlet spectra (measured at 100 K). STZ-white (at 100 K) provides the hydrohalite spectral endmember. Each mix represents an anhydrous percentage; 20% anhydrous corresponds to that measured in LH-Outlet by XRD at 20 °C. (a) Vis-NIR reflectance spectra of spectral endmembers and their mixes; (b) continuum-removed spectral mixes. Grey dashed lines denote the position of major hydrohalite band minima at 1452 and 1983 nm (visible in STZ-white).